# Elastomechanics of Lipid Membranes with Anisotropic Inclusions
# Studienarbeit

Ronald Holzlöhner
Arbeitsgruppe Prof. Hess
*TU Berlin, Institut für Theoretische Physik, Sekr. PN 7-1, Hardenbergstr. 36, 10623 Berlin*
(March 20, 1997)

Es wird die Elastomechanik von Lipidmembranen untersucht, die Einschlüsse in ihren Oberflächen tragen. Diese Einschlüsse krümmen die Membran und können so gewellte Strukturen hervorrufen, die experimentell beobachtet wurden. Andererseits sind sie aber auch vollkommen frei, sich auf der Membranoberfläche zu drehen und lateral zu bewegen, sodaß es zu Agglomerations- und Verarmungseffekten der Einschlüsse kommen kann. Es wird nun die freie Energie des Gesamtsystems bestimmt und ein Gleichgewichtszustand der Membran durch numerische Simulationen ermittelt.

## I. INTRODUCTION

Since Canham and Helfrich published some properties of lipid membranes in the early seventies [Helfrich73], these biological systems have attracted a great deal of interest both from experimental and theoretical physicists and chemists.

Lipid membranes consist of two layers of lipid molecules ("lipids"). A lipid molecule includes a hydrophilic head and a hydrophobic tail and has a length of some ten angstroms. Exposed to polar solvents, lipids tend to agglomerate in order to minimize their potential energies and either form micelles or bilayers, where only the heads are directed toward the solvent. Fluid bilayers can be thought of as 2D-fluids resembling soap films. The lipid molecules are free to move against each other just like soap molecules in a bubble shell. The difference is that lipid membranes hardly can vary their thickness since the constituting chains must remain aligned normal to the membrane plane and cannot pile up or extend significantly. The intermolecular distance is fixed to a small range; harsh stretching of the membrane simply results in tearing. For this reason, the surface area of a given fluid bilayer is roughly proportional to its total number of molecules and therefore practically constant, as long as the membrane cannot easily exchange lipids with a reservoir like a surrounding solution. As a consequence, lipid membranes adjust to an equilibrium surface area with zero surface tension.

Fluid membranes have a bending stiffness and thus behave like elastic shells. A free energy density of a pure membrane can be written as a function of the local principal curvatures. Since the energy may not change if we flip the membrane upside down (there cannot be uneven powers of the curvature), this reads to lowest order as

$$f(c_1,c_2) = \frac{\kappa}{2}(c_1+c_2)^2 + \tilde{\kappa}\, c_1 c_2 \,, \tag{1}$$

where $\kappa$ and $\tilde{\kappa}$ are the bending modulus and the Gaussian modulus, respectively [Helfrich73]. At room temperature, $\kappa$ ranges from the order of $k_BT$ for amphiphilic lipid membranes over $10 \ldots 100\, k_BT$ for longer lipids up to $10^4\, k_BT$ and more for membranes consisting of polymers. For later calculations of critical lengths and approximations, we will assume $\kappa \approx 20\, k_BT$ as a typical value.

The characteristic properties of constant total area, significant rigidity and often a very large lateral extent compared to its thickness make a sheet of paper a good macroscopic model for a lipid membrane. However, a lipid membrane has the additional capability of bulging by rearranging lipids, which paper has not. Geometrically speaking, this corresponds to a variation of the local intrinsic surface metric while keeping its average constant. (Incompressible 2D-fluid with constant thickness)

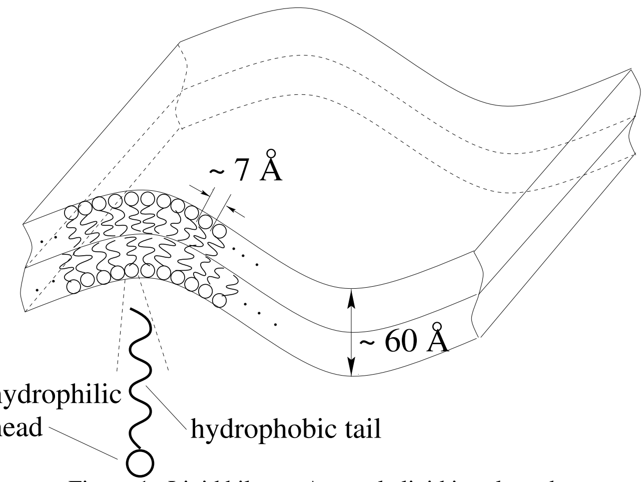


Figure 1. Lipid bilayer. A sample lipid is enlarged.

Statistical mechanics of pure lipid membranes have been investigated a lot, i.e. in [Goldstein89,Nelson]. Biological systems such as cell walls usually contain inclusions in the bilayers like proteins or imperfections such as two chemically bound lipids ("Gemini"). These impurities can prefer a finite spontaneous curvature and thereby induce a corrugated phase of the overall membrane. This has been studied both experimentally [Meyer90,Sternberg87] and theoretically [Lubensky93,Fournier96,GoetzDiplom,Goetz96]. Also, interaction energies between inclusions [Netz95] were investigated analytically.
However, these theories rarely took into account a special

shape of the inclusions, nor calculated the macroscopic conformation of a membrane carrying them as translational free impurities. Anisotropic inclusions, whose elastic energies depend on the rotation angle in the membrane plane, have not been considered until recently [Fournier96].

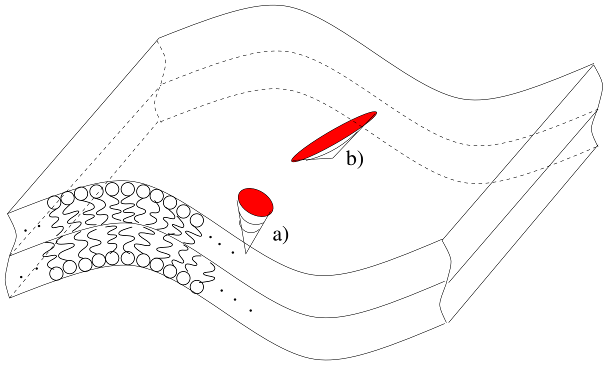


Figure 2. Lipid membrane with inclusions. Isotropic *(a)* and anisotropic *(b)* inclusions are distinguished.

## II. MODEL

We consider a lipid membrane consisting of two symmetric monolayers. Both layers can independently carry inclusions. Inclusions may not be exchanged between the monolayers, but are otherwise allowed to freely move on the membrane. They are assumed to be non-interacting, thus forming two adjacent ideal 2D-gases.

The questions we try to answer include the following:

- Which equilibrium shape will the membrane approach? What symmetries will it feature?
- Is there a phase transition such as a threshold for instabilities to arise? Where is it and what does it depend on? What order is it of?
- Are there qualitative differences between isotropic and anisotropic inclusions? In what way does the equilibrium shape depend on the anisotropy of the inclusions?
- Will a macroscopic system tend to equalize its shape and inclusion density on a large scale or rather develop flat, inclusion depleted areas and other, agglomerated domains? This effect would be due to interaction with the curvature field.

We now develop a continuous mean field theory to derive a Hamiltonian for the doped membrane [Fournier96].

### A. Length Scales

We consider a displacement field $u(x,y)$ of the membrane midplane where $x$ and $y$ are Cartesian coordinates. By this choice, we restrict ourselves to smaller slopes and especially exclude rolled-up conformations, i.e. vesicles and tubes.

Inclusions are assumed to be anisotropic and uniform. The orientation of a single inclusion can be described by a unit vector $\mathbf{a}$ in the plane $(x,y)$. As in a nematic liquid crystal, we assume oriented, but not directed inclusions (head-tail-symmetry), so only the dyad $\mathbf{aa}$ can be relevant at lowest order.

The inclusion energy depends on the local curvature of the bilayer. For small curvatures, this is approximately given by the tensor $\mathsf{U}_{ij} = \partial^2 u / (\partial x_i \partial x_j)$.

The energy of a single inclusion can be written as

$$E(\mathsf{U},\mathbf{aa}) = E_0 + \mathsf{T}_{ij}(\mathbf{aa})\,\mathsf{U}_{ij} + O(\mathsf{U}^2)\,, \tag{2}$$

with summation over repeated indices implied. This equation describes the inclusion contribution to the spontaneous curvature of the membrane. $\mathsf{T}_{ij}$ are linear functions of $\mathbf{aa}$. The tensor $\mathsf{T}$ can be decomposed in a term proportional to the identity $\mathbf{I}$ and a term proportional to $\overleftrightarrow{\mathbf{aa}} \equiv \mathbf{aa} - 1/2\,\mathrm{Tr}\,\mathbf{aa}\,\mathbf{I}$, the symmetric traceless part of $\mathbf{aa}$:

$$\mathbf{a} = \begin{pmatrix} \cos\vartheta \\ \sin\vartheta \end{pmatrix} \tag{3}$$

$$\begin{aligned} \overleftrightarrow{\mathbf{aa}} &= \begin{pmatrix} \cos^2\vartheta - \frac{1}{2} & \cos\vartheta\,\sin\vartheta \\ \cos\vartheta\,\sin\vartheta & \sin^2\vartheta - \frac{1}{2} \end{pmatrix} = \\ &= \begin{pmatrix} \frac{1}{2}\cos 2\vartheta & \cos\vartheta\,\sin\vartheta \\ \cos\vartheta\,\sin\vartheta & -\frac{1}{2}\cos 2\vartheta \end{pmatrix} \end{aligned} \tag{4}$$

The curvature tensor can be diagonalized, its eigenvalues are the local principal curvatures $c_1$ and $c_2$. Approximately, this also holds for $\mathsf{U}$. Defining $\vartheta$ as the angle between $\mathbf{a}$ and, say, the axis of curvature $c_1$, we are led to

$$\boxed{E(c_1,c_2,\vartheta) = E_0 + \underbrace{\alpha(c_1+c_2)}_{\text{isotropic}} + \underbrace{\omega(c_1-c_2)\cos 2\vartheta}_{\text{anisotropic}}} \tag{5}$$

in which we can choose $\omega > 0$ without loss of generality. $\alpha$ scales the isotropic energy contribution and $\omega$ the (purely) anisotropic.

A term linear in $c_1 \pm c_2$ like (5) also arises when incorporating inclusion contributions into (1) as

$$f = \frac{\kappa}{2}(c_1 + c_2 - c_0)^2 + \cdots \tag{6}$$

found i.e. in [Nelson,Netz95], where $c_0$ gives the ground state curvature induced by an inclusion. This can be seen by $(c_1+c_2-c_0)^2 \equiv (c_1+c_2)^2 + c_0{}^2 - 2c_0(c_1+c_2)$ ($c_0$ is constant).

A characteristic length of this system is given by the curvature radius at which thermal fluctuations overcome the tendency of the inclusions to orient along the most favorable axis, this is $\omega(c_1-c_2) \approx k_B T$. We define here

$$\frac{1}{c^\star} \equiv \frac{\omega}{k_B T} \tag{7}$$

An analogous length scale can be given for isotropic systems:

$$R \equiv \frac{1}{c^\dagger} \equiv \frac{\alpha}{k_B T} \tag{8}$$

We estimate $R$. Suppose, a wedge-shaped inclusion is embedded in the membrane, as shown in Fig. (3). We like to find out about the ratio between $R$ and $a$, where $a$ is the head size of a lipid molecule. Suppose the tilt of the inclusion neighboring lipids relaxes within a few molecule sizes. Then

$$\theta_1 = \frac{d+a}{2}\,\frac{1}{R} \tag{9}$$

A circle-shaped inclusion should be surrounded by $N \approx \pi(d+a)/a$ lipids, all of them having a single energy of $h_{single} = k_B T \theta_1/\theta_{therm}$, where $\theta_{therm}$ is the 'thermal' angle that would cause an elastic tilt energy of $k_B T$. It is experimentally known that $\theta_{therm} \approx 20° \approx 1/3$, which is not very much. This results in

$$\begin{aligned} k_B T \approx N\, h_{single} &= \frac{\pi}{2aR}(d+a)^2 \frac{k_B T}{\theta_{therm}} \\ \Longrightarrow \frac{R}{a} &= \frac{1}{ac^\dagger} \approx \frac{1}{2}\left(1+\frac{d}{a}\right) \gg d, a \end{aligned} \tag{10}$$

provided that the entire inclusion causes itself an elastic tilt energy of $k_B T$ and has a size much larger than a head size. This should be the case for phospholipid membranes and large head detergent dimers as inclusions. Therefore, expected curvature radii range around $50\ldots200\,nm$. Since this is also a lot larger than the membrane thickness of ca. $6\,nm$, we have a justification for not going to higher order in the curvature tensor in (2).

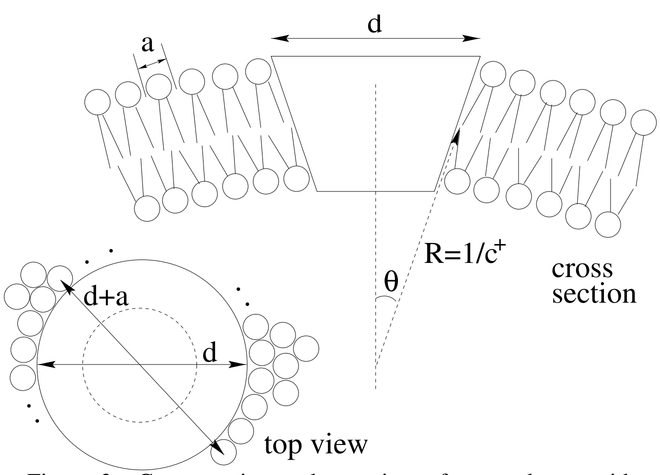


Figure 3. Cross section and top view of a membrane with a wedge-like inclusion. The resulting curvature radius is depicted.

**B. Membrane Free Energy**

The statistical physics of two lattice gases of oriented particles that couple to a curved surface is rather complex [Goulian95,Golestanian96,Netz95]. The following ansatz relies on a mean field simplification of the rotation angles, which are just thermally summed over.

If we neglect interaction energies between inclusions, the free energy of a single inclusion in a given shape derived from (5) is (This paragraph is adapted from [Fournier96])

$$\begin{aligned} F_1(c_1,c_2) &= -k_B T \ln Z = E_0 + \alpha(c_1+c_2) \\ &\quad - k_B T \ln \int_0^{2\pi} \frac{\mathrm{d}\vartheta}{\vartheta_0}\, e^{-\frac{\omega}{k_B T}(c_1-c_2)\cos 2\vartheta}\,, \end{aligned} \tag{11}$$

where $\vartheta_0$ is an irrelevant angle as it just adds a constant contribution to the total energy.

The integral in (11) results in a modified Bessel function $2\pi\vartheta_0^{-1}\ln \mathrm{I}_0((c_1-c_2)/c^\star)$. The total contribution of the inclusions to the membrane free energy density, $g_{incl}(c_1,c_2)$, is given by $nF_1(c_1,c_2)+nF_1(-c_1,-c_2)$, since inclusions on opposite sides of the bilayer experience opposite curvatures. We obtain

$$g_{inc}(c_1,c_2) = -2nk_B T \ln \mathrm{I}_0\left[\frac{c_1-c_2}{c^\star(T)}\right], \tag{12}$$

in which we eliminated a constant contribution, namely $nE_0 - nk_B T \ln(2\pi/\vartheta_0)$, that includes the rotational entropy of the inclusions. As expected in a symmetric bilayer, the term proportional to $(c_1+c_2)$ disappears, however the contribution resulting from the anisotropy remains. A graph of $g$ is shown in Fig. 4.

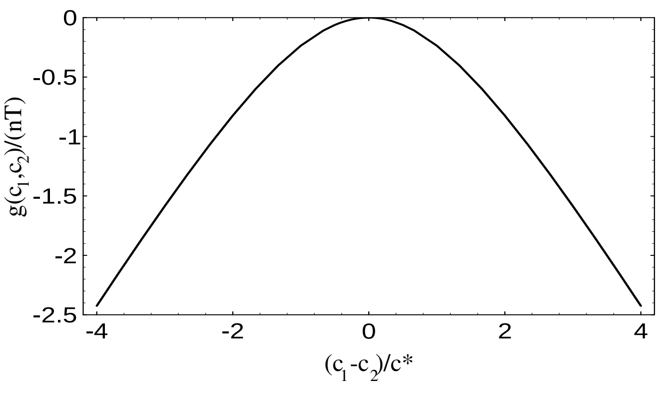


Figure 4. Free energy contribution of the inclusions. For $c_1 - c_2 \gg c^\star$, $g$ is almost linear.

The membrane bending energy is obtained by adding the contribution $g_{incl}(c_1,c_2)$ to the Helfrich energy (1). We consider two limits:

*a)* $|c_1 - c_2| \lesssim c^\star$—If the deviatoric bending is smaller than the threshold $c^\star$, the inclusions contribution simply renormalizes the membrane bending moduli. From $g(c_1,c_2) \sim -\frac{1}{4}n(k_BT)^{-1}\omega^2(c_1-c_2)^2 + O((c_1-c_2)^4)$, we derive

$$\Delta\kappa = -\frac{n\omega^2}{2k_BT} \tag{13a}$$

$$\Delta\tilde{\kappa} = \frac{n\omega^2}{k_BT}\,. \tag{13b}$$

Hence, the bending modulus $\kappa$ is reduced, as is usually the case for cosurfactants [Israelachvili]. Furthermore anisotropic inclusions favor *negative* Gaussian curvature (i.e., saddle shapes), as will be made clearer in the following.

*b)* $|c_1 - c_2| \gtrsim c^\star$—If the deviatoric bending is larger than $c^\star$, which is possible for large inclusions, $g$ becomes approximately

$$g(c_1,c_2) \sim nA - n\omega|c_1-c_2|\,, \tag{14}$$

where $A = \frac{1}{2}k_BT\ln[2\pi|c_1-c_2|/c^\star]$ can be treated as a constant thanks to its weak logarithmic dependence. This linear behavior can be easily understood from a mean field picture. According to Eq. (5), the orientation of minimum energy for a single inclusion corresponds to $\vartheta = 0$ if $c_1 - c_2 < 0$ and to $\vartheta = \pi/2$ if $c_1 - c_2 > 0$. In both cases, the anisotropic energy contribution is exactly $\omega|c_1-c_2|$. Since $c_1 - c_2$ changes sign from one monolayer of the membrane to the other, anisotropic inclusions will orient at right angles when the membrane is shaped as a saddle. This corresponds to the most favorable situation (Fig. 5). Conversely, if the membrane is shaped as a sphere, there is exact compensation on the two sides of the bilayer. Thus, in contrast with the usual Gaussian curvature term $\tilde{\kappa}c_1c_2$, the presence of anisotropic inclusions provides an energy gain within the saddles that is *not* compensated by a corresponding energy loss in surrounding 'hats'. In other words, the Gauß-Bonnet theorem does not apply to Eq. (14). This property was first understood by T. M. Fischer, who postulated by analogy with the spontaneous mean curvature a term proportional to $|c_1-c_2|$ for pure membranes, but estimated it to be negligible [FischerIII,FischerV].

The Gauß-Bonnet theorem states that for any simple connected surface $S$ surrounded by a closed smooth curve $\mathbf{r}(s)$ parametrized by arc length running on $\partial S$ with arc length $s$ the equation

$$\oint_{\partial S} c_g\,\mathrm{d}s + \underbrace{\iint_S c_1c_2\,\mathrm{d}S}_{\text{total curvature}} = 2\pi \tag{15}$$

holds true. $c_g$ is the projection of the curvature vector of $\mathbf{r}(s)$ on $S$:

$$\frac{\mathrm{d}^2\mathbf{r}}{\mathrm{d}s^2} = c_N\,\mathbf{N} + c_g\left(\mathbf{N}\times\frac{\mathrm{d}\mathbf{r}}{\mathrm{d}s}\right) \tag{16}$$

($\mathbf{N}$ is the unit normal of $S$). For closed or periodic surfaces this means that the total curvature is constant.

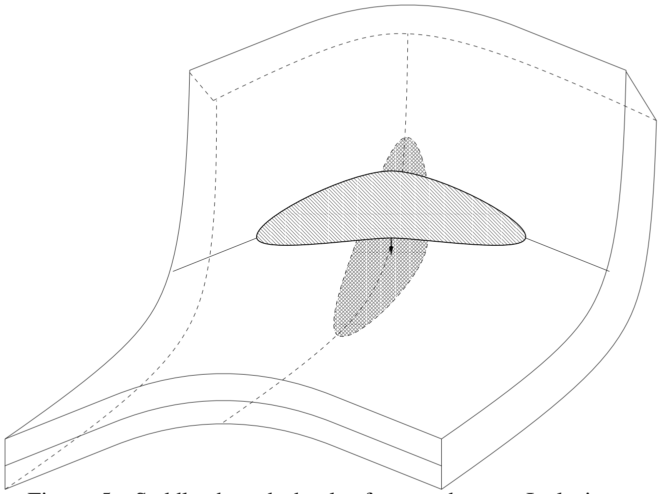

Figure 5. Saddle-shaped chunk of a membrane. Inclusions on opposite surfaces of the membrane are oriented in right angles to each other at $T = 0$.

### C. Local Inclusion Densities

As mentioned before, we want to treat the inclusions as two ideal lattice gases on the membrane. Thus, we have to deal with two inclusion densities $n_{upper}$ and $n_{lower}$. It turns out that it is more convenient to rather take the sum and difference of the density perturbations from uniform distribution:

$$n_{upper} \equiv n_0(1+\phi+\psi)\,, \qquad n_{lower} \equiv n_0(1+\phi-\psi) \implies$$
$$\phi = \frac{n_{upper}+n_{lower}}{2n_0} - 1\,, \qquad \psi = \frac{n_{upper}-n_{lower}}{2n_0}$$

In these terms, we do obtain an isotropic energy contribution and a coefficient of $(1+\phi)$ for the anisotropic term:

$$g = \frac{\kappa}{2}(c_1+c_2)^2 + \\ + 2n_0\left[\alpha(c_1+c_2)\psi - k_BT(1+\phi)\ln\mathrm{I}_0\left(\frac{c_1-c_2}{c^\star}\right)\right] \tag{17}$$

The Gaussian curvature term was omitted in consideration of the Gauß-Bonnet theorem. Of course, this is only valid for constant topologies.

The isotropic part of (17) energetically favors curvatures of different sign than the density difference $\psi$ (i.e. more inclusions on top of a summit than under it).

$\ln\mathrm{I}_0(\cdot)$ as an even and non-negative function corresponds to anisotropic inclusions which are happy in saddles with high mutual inclusion densities.

Note that purely isotropic inclusions only can undulate a membrane by having more particles on one layer than on the other ($\psi \neq 0$), while anisotropic inclusions can already induce this with constant density.

It should be said that the picture of two independent gases is not to be taken too literally. If we consider inclusions of several head sizes, it is unrealistic to assume they would not extend over both monolayers. However, if inclusions are wedge-shaped, they cause a local isotropic effect. In our notation, this can be expressed by two different single inclusion densities at this point, giving in a way its lateral extent measured on the two sides separately. In this case, the $\psi$–field is limited since the $\phi, \psi$–fields are not independent anymore.

### D. Translational Entropy

In a free lattice gas, we also encounter a translational entropy. To derive it here, we have to answer the following question:

For a fixed average inclusion density $n_0$, what is the probability for a small subpart $\widehat{A}$ of the membrane $A$ to carry a different number of particles $\widehat{N} = (1+\epsilon)\langle\widehat{N}\rangle$ than the expectation value $\langle\widehat{N}\rangle = n_0\widehat{A}$ ($n_0 \equiv \langle\widehat{n}\rangle$: avg. incl. density) ? For a large total number of particles $N$ and a small sample part this is according to Poisson

$$\mathcal{P}_N(\widehat{N}) = \frac{\langle\widehat{N}\rangle^{\widehat{N}}\ \mathrm{e}^{-\langle\widehat{N}\rangle}}{\widehat{N}!} \overset{\widehat{N}\gg 1}{\approx} \left(\frac{\langle\widehat{N}\rangle}{\widehat{N}}\right)^{\widehat{N}} \mathrm{e}^{\widehat{N}-\langle\widehat{N}\rangle} \tag{18}$$

Or, going in the above limit over to densities

$$\widehat{N} \to \widehat{n} \equiv \frac{\widehat{N}}{\widehat{A}}, \qquad \langle\widehat{N}\rangle \to n_0 \equiv \langle\widehat{n}\rangle = \frac{N}{A}$$

$$\mathcal{P}_{n_0}(\widehat{n}) \approx \left(\frac{n_0}{\widehat{n}}\right)^{\widehat{n}} \mathrm{e}^{\widehat{n}-n_0} \qquad \Longrightarrow$$

$$\begin{aligned} S &= k_B \log \mathcal{P}_{n_0}(n_0(1+\epsilon)) = \\ &= k_B n_0\Big[(1+\epsilon)\log(1+\epsilon) - \epsilon\Big] = k_B n_0 \left[\frac{\epsilon^2}{2} + O(\epsilon^3)\right] \end{aligned} \tag{19}$$

Writing (19) in terms of $\phi$ and $\psi$–fields ($\epsilon \equiv \phi \pm \psi$), we obtain an expression for the translational entropy with a minimum at the equilibrium density at $n = n_0$:

$$\begin{aligned} S = k_B n_0 s = k_B n_0 \,[ &(1+\phi+\psi)\log(1+\phi+\psi) + \\ + &\ (1+\phi-\psi)\log(1+\phi-\psi) - 2\phi] \end{aligned} \tag{20}$$

which is expanded up to second order:

$$\begin{aligned} k_B n_0 \frac{\epsilon^2}{2}\bigg|_{\epsilon=(\phi\pm\psi)} &= k_B \frac{n_0}{2}\left((\phi+\psi)^2 + (\phi-\psi)^2\right) \\ &= k_B n_0(\phi^2+\psi^2) \end{aligned} \tag{21}$$

### E. Linear Stability Analysis

In order to find a critical average inclusion density $n_{0,crit}$ for conformational instabilities to arise, we employ a linear stability analysis in the total free energy where terms of higher order than two were neglected and with the usual approximation $c \approx \partial^2 u(x)/\partial x^2 \equiv u''(x)$. We restrict the calculation to the onset of cylindrical waves, this means translational invariance in $y$ –direction, $c_2 \equiv 0$.
The linearized free energy looks like:

$$\begin{aligned} \tfrac{G}{n_0} &= \int_0^L \frac{1}{n_0}\frac{\kappa}{2}(u'')^2 + k_B T\left(\phi^2+\psi^2\right) + \\ &\quad +2\Big[\alpha c\psi - k_B T \underbrace{\ln \mathrm{I}_0\left(\frac{u''}{c^\star}\right)}_{\approx 1/4\,(u''/c^\star)^2}\Big]\,\mathrm{d}x = \\ &= \int_0^L \underbrace{\frac{1}{2}\Big(\frac{\kappa}{n_0} - \frac{k_B T}{c^{\star 2}}\Big)}_{\equiv Q}(u'')^2 + k_B T(\phi^2+\psi^2) + 2\alpha\psi u''\ \mathrm{d}x \end{aligned}$$

where $u'' \approx c = c_1 + c_2 = c_1 - c_2$. The coefficient $(1+\phi)$ in the anisotropic term in (17) was neglected to prevent from third powers in $\phi$. The three fields $u(x), \phi(x), \psi(x)$ are expressed as Fourier series:

$$u(x) = \sum_k U_k\ \mathrm{e}^{ikx}\ ,$$

$$\phi(x) = \sum_k \Phi_k\ \mathrm{e}^{ikx}\ ,\quad \psi(x) = \sum_k \Psi_k\ \mathrm{e}^{ikx}$$

Keeping in mind that these fields are real ($u = u^\star$ etc.) , the transformed free energy reads

$$\begin{aligned} \frac{\widehat{G}}{n_0} &= \sum_k Qk^4|U_k|^2 + k_B T\left(|\Phi_k|^2 + |\Psi_k|^2\right) - \alpha k^2\big(U_k\Psi_k^\star + U_k^\star\Psi_k\big) \\ &= k_B T\left[|\Phi_k|^2 + |\Psi_k - \frac{\alpha k^2}{k_B T}U_k|^2\right] + k^4\left[Q - \frac{\alpha^2}{k_B T}\right]|U_k|^2 \end{aligned} \tag{22}$$

Since magnitudes are non-negative, the instability condition reduces to the last bracket:

$$\frac{1}{2}\left(\frac{\kappa}{n_0} - \frac{k_B T}{c^{\star 2}}\right) < \frac{\alpha^2}{k_B T} \iff \boxed{n_{0,crit} = \frac{k_B T\kappa}{2\alpha^2 + \omega^2}} \tag{23}$$

Larger values for $n_0$ than $n_{0,crit}$ lead to some sort of corrugated phase, below this, the membrane remains flat except for thermal fluctuations. (23) shows that the onset depends linearly on $\kappa$. Moreover, we notice that instabilities arise earlier for mixed than for isotropic systems which is not surprising. It is convenient to rewrite the free energy density in terms of normalized variables, as shown in the next section.

This critical inclusion density $n_{0,crit}$ also provides a basis for an estimation of the ratio between number of particles and critical area: If $\kappa \geq 20\ k_B T$, we get for isotropic systems

$$n_{0,crit} \geq \frac{10\,(k_B T)^2}{\alpha^2} = 10\,c^{\dagger\,2}, \tag{24}$$

Hence we can expect more than 10 inclusions per squared critical length or $(2\pi)^2 \times 10 \approx 400$ per squared wavelength of a sine-shaped undulation with critical curvature in the extrema. This is a good justification for a continuous model.

### F. Normalized Variables

We define the following variables:

$$\overline{c_+} \equiv \frac{c_1 + c_2}{c^\dagger}\ , \qquad \overline{c_-} \equiv \frac{|c_1 - c_2|}{c^\dagger}$$
$$\Gamma \equiv \frac{\omega}{\alpha} = \frac{c^\dagger}{c^\star}$$

The quantity $\Gamma$ gives the ratio of the (purely) anisotropic to the isotropic energy contribution (zero for isotropic systems). The un-reduced free energy density again reads

$$\begin{aligned} g = &\frac{\kappa}{2}(c_1+c_2)^2 + n_0 k_B T\, s + \\ &+ 2n_0\left[\alpha(c_1+c_2)\psi - k_B T(1+\phi)\ln \mathrm{I}_0\left(\frac{c_1-c_2}{c^\star}\right)\right] \end{aligned} \tag{25}$$

Normalize this by $\kappa {c^\dagger}^2$:

$$\overline{g} \equiv \frac{g}{\kappa {c^\dagger}^2}\ , \qquad \overline{n_0} \equiv 2\frac{n_0 k_B T}{\kappa {c^\dagger}^2} \tag{26}$$

where $\overline{n_0}$ is defined such that $\overline{n_0}(n_{0,crit}) = 1$ for isotropic systems. This yields i.e. for the Helfrich term:

$$\frac{\kappa}{2}(c_1+c_2)^2 \cdot \frac{1}{\kappa {c^\dagger}^2} \equiv \frac{1}{2}\overline{c_+}^2$$

Of special interest is the anisotropy term:

$$-2n_0 k_B T\ \ln \mathrm{I}_0\left(\frac{c_1-c_2}{c^\star}\right) \cdot \frac{1}{\kappa {c^\dagger}^2} = -\overline{n_0}\ln \mathrm{I}_0\Big(\underbrace{\frac{c_1-c_2}{c^\dagger}}_{\equiv\overline{c_-}}\ \underbrace{\frac{c^\dagger}{c^\star}}_{\equiv\Gamma}\Big)$$

In all what follows below we now omit the bars for the sake of simplicity:

$$\boxed{g = \frac{{c_+}^2}{2} + \frac{n_0}{2}s + n_0\Big[\underbrace{c_+\psi}_{\text{isotropic}} - \underbrace{(1+\phi)\ln \mathrm{I}_0(c_-\Gamma)}_{\text{anisotropic}}\Big]} \tag{27}$$

This notation makes it easy to see that this new $n_0$ $(\equiv \overline{n}_0)$ can be thought of as an effective inverse bending rigidity (more inclusions soften the membrane, as usual). The difference of curvatures $c_-$ $(\equiv \overline{c_-})$ is scaled by $\Gamma$.

### G. Variational Calculus

To find the equilibrium conformation of the membrane, we have to deal with a 3-field problem, namely $u(x,y)$, $\phi(x,y)$, $\psi(x,y)$.

We want to minimize

$$G = \frac{1}{A}\iint_0^L g\ \mathrm{d}\sigma \tag{28}$$

with

$$A = \iint_0^L \mathrm{d}\sigma\ , \qquad \mathrm{d}\sigma \equiv \sqrt{1+{u_x}^2+{u_y}^2}\,\mathrm{d}x\,\mathrm{d}y$$
$$u_x \equiv \frac{\partial u(x,y)}{\partial x}\ , \qquad u_y \equiv \frac{\partial u(x,y)}{\partial y}$$

with $A$ the membrane surface area and $\sigma^2$ the local surface metric. The natural way would be to find Euler-Lagrange equations for all three fields. Because of the essential nonlinearity of the $\ln \mathrm{I}_0(\cdot)$ function and the complicated terms that would occur in the derivatives of the curvatures, we restrict this here to the density perturbations $\phi, \psi$. Since they must be zero on average, we run into two isoperimetric conservation conditions

$$\iint_0^L \phi\ \ \mathrm{d}\sigma = 0\ , \qquad \iint_0^L \psi\ \ \mathrm{d}\sigma = 0 \tag{29}$$

These must be accounted for by two Lagrangian multipliers $\Lambda_\phi, \Lambda_\psi$, giving the new free energy density $g_\Lambda$ which replaces the $g$ to minimize in (28):

$$\begin{aligned} g_\Lambda &\equiv g + \Lambda_\phi\phi + \Lambda_\psi\psi = \\ &= \frac{{c_+}^2}{2} + \frac{n_0}{2}\Big[\phi^2+\psi^2\Big] + n_0\Big[c_+\psi - \ln \mathrm{I}_0(c_-\Gamma)\Big] \\ &\quad + \Lambda_\phi\phi + \Lambda_\psi\psi \end{aligned} \tag{30}$$

(Again, the quadratic entropy term $s \approx \phi^2+\psi^2$ was taken.) Then, we find the two Euler-Lagrange equations:

$$g_{\Lambda,\phi}\ -\ \frac{\mathrm{d}}{\mathrm{d}l}g_{\Lambda,\phi'} = 0 \qquad \left(\phi' \equiv \frac{\partial\phi}{\partial l}\ ,\ g_{\Lambda,\phi} \equiv \frac{\partial g_\Lambda}{\partial\phi}\dots\right)$$
$$\Longrightarrow \quad \phi_{eq} = \ln \mathrm{I}_0(c_-\Gamma) - \frac{\Lambda_\phi}{n_0} \tag{31a}$$
$$g_{\Lambda,\psi}\ -\ \frac{\mathrm{d}}{\mathrm{d}l}g_{\Lambda,\psi'} = 0 \qquad \left(\psi' \equiv \frac{\partial\psi}{\partial l}\right)$$
$$\Longrightarrow \quad \psi_{eq} = -c_+ - \frac{\Lambda_\psi}{n_0} \tag{31b}$$

where $l$ is the arc length in one dimension. We have to obey to the conditions

$$\Lambda_\phi = \ \frac{n_0}{L}\int_0^L \ln \mathrm{I}_0(c_-\Gamma)\ \mathrm{d}l \qquad (>0) \tag{33}$$
$$\Lambda_\psi = -\frac{n_0}{L}\int_0^L c_+\ \mathrm{d}l \qquad (\approx 0) \tag{34}$$

Because $\ln \mathrm{I}_0(\cdot)$ is a non-negative function, condition (33) will yield a finite $\Lambda_\phi$. In contrast, $\Lambda_\psi$ will be small in most cases (zero for all symmetric $u(x,y)$).

A major complication is the local constraint $\phi \pm \psi \geq -1$ (to prevent from local negative densities), which is very hard to account for analytically.

### H. Segregation

An immediate question when trying to solve the problem is: Can we expect a periodic solution or would a macroscopic system tend to phase-separate? Here is a stability argument for small perturbations:
Suppose, we have a membrane much larger in lateral extent than $2\pi R$. Will it try to split in say, two domains with different inclusion densities? Imagine the $\phi$-field (sum of upper and lower relative inclusion densities) is increased by a constant $\Delta\phi$ in region A to $\phi+\Delta\phi$ and decreased to $\phi-\Delta\phi$ in region B. If A and B are equal otherwise, this means the net inclusion density $n_0$ and conditions (29) are still valid for both areas combined. Taking a look at (27), we find the effected terms:

$$\Delta G_{\mathsf{A,B}} = \frac{n_0}{A}\iint_0^L \frac{1}{2}\left(\pm\, 2\phi\,\Delta\phi + (\Delta\phi)^2\right) \mp \Delta\phi \ln \mathrm{I}_0(c_-\Gamma)\ \mathrm{d}\sigma$$

It is easy to see that the two effects have opposite signs for all terms with linear $\Delta\phi$ and therefore cancel each other. The quadratic term is positive for both A and B.
According to this, a homogeneous system is stabilized against small fluctuations in inclusion numbers by the entropy. However, reality is as usual a little more complicated: In the above argument, a periodic height field $u(x,y)$ is implied. Moreover, larger fluctuations also could include a migration of lipids which would result in some flat(ter) domains and others with more excess area and different wavelengths. This is far more complicated and should be covered by a simulation of a two-region system.

## III. NUMERICAL SIMULATION

The constraint of constant surface extent makes the problem of minimizing (28) hard to tackle analytically. Also, such approaches could only focus on one of the two regimes of simplifying $\ln \mathrm{I}_0(\cdot)$ (see Fig. 4). Methods can be based on assuming a periodic displacement field $u(x,y)$ which is reasonable at least on a mesoscopic scale of a few $R$. Then density perturbation fields are chosen i.e. according to rules (31a, 31b) and (global) minima of G are searched.
Test functions for $u(x,y)$ should include both egg-cartons and cylindrical waves and possibly crossover shapes. We take

$$u(x,y) = U(m)\left(\cos(2\pi\frac{x}{L_x}) + p\,\cos(2\pi\frac{y}{L_y})\right) \tag{35}$$

here. Note that the amplitude $U$ is determined by the constant ratio

$$m \equiv \frac{A}{L_x L_y}$$

of surface area $A$ to projected area, so the function space from which the $u(x,y)$ are picked is reduced to three dimensions $\{L_x, L_y, p\}$.
A first try was now to do a fourth-order Landau expansion of (27) in $U$. For the above mentioned difficulties this is complicated and gives finite results only on a rather limited parameter range.

The next approach was to numerically find minima for the above problem in the $\{L_x, L_y, p\}$ – space. This was checked against one-dimensional minimizations of symmetric 2D ‘egg-cartons’ ($p = 1$, $L = L_x = L_y$) and cylinder waves ($p = 0$). For the fields $\phi,\psi$, the results of (31a, 31b) were inserted and clipped if necessary so that always $\phi \pm \psi \geq -1$ would be obeyed. When varying $L_x, L_y$, always one full wavelength was kept in the box and periodic boundary conditions were maintained – only the scaling factor was changed. A standard multi-dimensional minimizing algorithm was used.

For some parameter combinations, this was verified by a Monte-Carlo simulation described further down.

### A. Results

The result of the three-dimensional minimization shows always $p = 1$, these are egg cartons. This is an important result and not obvious for isotropic systems which do not profit from saddles.

In Fig. a-c, only symmetric egg cartons and cylinder waves are compared (where the egg cartons are the global energy minimum in the $\{n_0, \Gamma, m\}$ – parameter space)

- Fig. a shows the graphs of $L(n_0)$ and $G(n_0)$ for cylinder waves and egg cartons. ($\Gamma = 1$, $m = 1.5$, $n_{0,crit} = 2/3$) A lot of interesting properties of the system are exhibited. Firstly, the curves of $L$ diverge for $n_0 \searrow n_{0,crit}$ ($= 2/3$ for $\Gamma = 1$); the Helfrich term then becomes predominant. For $n_0 \leq n_{0,crit}$, no energy minimum can be found with finite $L$, as expected.

  There is very little difference between the 1D and 2D wavelengths. For larger $n_0$, $L$ becomes of the order of 1 (always measured in units of $2\pi R$), so the extremal membrane curvatures are close to $c^\dagger$, as expected. The egg carton energies and wavelengths are always lower than for 1D waves, especially for larger $n_0$, where the saddle-friendly term $\ln \mathrm{I}_0(\cdot)$ is happy.

- Fig. b: Like Fig. a, but for $L(\Gamma), G(\Gamma)$. Larger values of $\Gamma$ soften the membrane as smaller of $n_0$ do. Here again both energies and wavelengths are lowest for egg cartons. ($n_0 = 1.75$, $m = 1.5$)

- Fig. c: Like Fig. a, but for $L(m), G(m)$. Larger $m$ provide additional membrane surface which results in higher average curvatures, so systems with much excess area also have big wavelengths. The effect is almost linear for $m > 1.3$. ($n_0 = 1.75$, $\Gamma = 1$)

The linear dependence $L(m)$ can be understood by calculating $m$ as the average of local surface metrics:

$$m \equiv \frac{1}{L^2} \iint_0^L \sqrt{1 + {u_x}^2 + {u_y}^2}\ \mathrm{d}x\,\mathrm{d}y$$

which shows that $m$ scales linearly with $u$ at large amplitudes and therefore at high curvatures.

The reason for the discontinuous leaps in the graphs is probably the existence of various local minima in $G(\cdot)$, which exchange the role of the global minimum.

### B. Monte-Carlo Simulation

An algorithm similar to a Monte-Carlo (MC) simulation with simulated annealing [GoetzDiplom,Goetz96] was carried out on a lattice with periodic boundary conditions. The purpose was to find the average membrane conformation at room temperature. This can either be be done by searching the global minimum of the free energy $G$, or performing an MC simulation of the doped membrane i.e. as a canonical ensemble. In the latter case, one needs to take the Hamiltonian rather than the free energy for simulating (omit the entropy) and average the shape over many timesteps.

Here, the first method with a non-deterministic 'thermal' approach was chosen, which makes it easier to avoid getting stuck in local minima. Unlike with 'real' MC, the free energy (27) containing an entropy term was taken for minimization rather than a pure Hamiltonian. The reason is that you artificially have to maintain fluctuations at room temperature when $k_BT$ is lowered in the simulation, as explained below.

The main advantage to the past section is that we do not restrict any variables like in (35) or linearize as in (31a, 31b).

A membrane represented by continuous values of $u(x,y)$, $\phi(x,y)$, $\psi(x,y)$ (Monge rep.) was simulated on a $40 \times 40$ – lattice. We started at random shape and high temperature, then 'cooled' the system slowly down until fluctuations almost vanished, the Metropolis acceptance rate was kept around 50 %. $10^5$ to $10^6$ steps were performed.

*Algorithm:* The lattice is initialized with a random shape that has surface excess $m$. $\phi$ and $\psi$ are set to zero. Then we choose random pairs of non-adjacent sites in a way that each site is visited exactly once per sweep.
Random perturbations of $u_{ij}, \phi_{ij}, \psi_{ij}$ out of intervals $[u_{ij} - \Delta u, u_{ij} + \Delta u]$ etc. are chosen. At the other site in the current pair, inverse perturbations are picked so that the changes in surface area and particle numbers are approximately compensated. (When compensating $\phi, \psi$, also different local $m_{ij}$ must be taken into account since the inclusion *numbers* on site $(ij)$ are $N_{ij} = m_{ij} n_0 (1 + \phi_{ij} \pm \psi_{ij})$. This is a 'surface-exchanger' algorithm: Always two sites are changed in one step in a way that the change in local area at one site is compensated by the other. The combined change is either accepted or rejected. This is known as "Kawasaki dynamic". This procedure is slow, but needs no surface dependent term in $g$. Inclusions are exchanged in the same manner, thus keeping their total number constant. Also the conditions $\phi \pm \psi \geq -1$ are to be observed. The entire operation is accepted upon the usual Metropolis criterion

$$\mathrm{e}^{-\frac{\Delta g_{ij}}{k_B T}} > \texttt{random(0,1.0)} \tag{36}$$

The perturbation widths $\Delta u, \Delta\phi, \Delta\psi$ are varied so that always an acceptance rate of around 50 % is maintained.
Throughout the whole process, the temperature as it appears in (36) is lowered successively. The starting $k_BT$ ranges around several times of the Helfrich term ${c_+}^2/2$ and is repeatedly divided by a constant factor until the average changes in energy $\Delta g_{ij}$ fall below a certain limit. This does not mean the *physical* temperature is lowered to zero; the free energy is still calculated at room temperature. Only the tendency to leave a found minimum is reduced.

It is possible [6] to link the changes in temperature to the current heat capacity of the system, which can be significantly lowered when decreasing temperatures (and so the ensemble becomes more sensitive to changing $T$). However, this is not implemented here.

An output of the MC simulation is shown is Fig. d.

## IV. LIMITATIONS

These results are only valid for non-interacting particles and on a scale of few wavelengths, since macroscopic systems might want to form multiple phases (See section II H). Also, in case of large anisotropic energy contributions the mean field calculation becomes problematic and we have to consider an inclusion director field. The problem is the assumption of (11), where the sum in the partition function is only taken over the rotation angles. The corresponding statistical ensemble does not exactly describe a lattice gas of particles, whose rotational degrees of freedom have the same weight as the translational ones. 'Nematic' phases of anisotropic inclusions (collective alignment) cannot be described.

We neglect inclusion-inclusion interactions as in [Netz95] by taking densities of independent particles.

## V. SUMMARY

A free energy expression (27) is found for bending elastic membranes carrying oriented, laterally and rotationally mobile inclusions. These systems are characterized by $n_0, \Gamma$ and $m$. Critical lengths (10) and inclusion densities (23) are calculated. A periodic equilibrium state is numerically searched for with given parameter sets.

I wish to thank J.B. Fournier, currently at ESPCI Paris, Phil Pincus (UC Santa Barbara), Martin Schoen and Martin Kröger for a lot of helpful discussions. C. Jeppesen (UCSB) gave me much support on details of the MC simulation.

* Ronald Holzlöhner, TU Berlin, Institut für Theoretische Physik, Hardenbergstr. 36, 10623 Berlin, e-mail: *ronald@physik.tu-berlin.de*

$Helfrich73$ P. Canham, J. Theor. Biol. **26**, 61 (1970), W. Helfrich, *"Elastic Properties of Lipid Bilayers"*, Z. Naturforsch. **28c**, 693-703 (1973)

$Israelachvili$ J. N. Israelachvili, *"Intermolecular and Surface Forces"*, (Academic Press, London 1992)

$Nelson$ D. Nelson *et al.* editors, *"Statistical Mechanics of Membranes and Surfaces"*, (World Scientific, Singapore 1989)

$Meyer90$ W. Meyer, W. Richter, J. Gumpert, Bioch. et Biophys. Acta, **1026**, 171-8 (1990)

$Sternberg87$ B. Sternberg, J. Gumpert *et al.*, Bioch. et Biophys. Acta, **898**, 223-30 (1987)

$Goldstein89$ R. Goldstein, S. Leibler, *"Structural Phase Transitions of Interacting Membranes"*, Phys. Rev. A **40**, 1025-34, (1989)

$Lubensky93$ T.C. Lubensky, F.C. MacKintosh, *"Theory of Ripple Phases of Lipid Bilayers"*, Phys. Rev. Lett. **71**, 1565-68 (1993)

$Fournier96$ J.B. Fournier, *"Nontopological Saddle-Splay and Curvature Instabilities from Anisotropic Inclusions"*, Phys. Rev. Lett. **76**, 4436-39 (1996)

$Netz95$ R. Netz, P. Pincus, *"Inhomogeneous Fluid Membranes: Segregation, Ordering and Effective Rigidity"*, Phys. Rev. E **52**, 4114-27 (1995)

$Goulian95$ M. Goulian, R. Bruinsma, P. Pincus, *"Long-Range Forces in Heterogeneous Fluid Membranes"*, Europhys. Lett. **22**, 145-50 (1993)

$Golestanian96$ R. Golestanian, M. Goulian, M. Kardar, *"Fluctuation-Induced Interactions between Rods on Membranes and Interfaces"*, Europhys. Lett. **33**, 241-5 (1996)

$CaiNelson93$ W.Cai, T.C. Lubensky, P. Nelson and T. Powers, *"Measure Factors, Tension and Correlations of Fluid Membranes"*, Preprint

$FischerIII$ T. M. Fischer, *"Bending Stiffness of Lipid Bilayers. III. Gaussian Curvature"*, J. Phys. II France **2**, 337 (1992)

$FischerV$ T. M. Fischer, J. Phys. II France **3**, 1795 (1993)

$GoetzDiplom$ Rüdiger Goetz, *"Monte-Carlo-Simulation einer Überstruktur auf Lipidmembranen"*, Diplomarbeit, (1993)

$Goetz96$ Rüdiger Goetz, W. Helfrich, *"The Egg Carton: Theory of a Periodic Superstructure of Some Membranes"*, J. Phys. II France, **6**, 215-223 (1996)

[1] L.E. Reichl, *"A Modern Course in Statistical Physics"*, (Univ. of Texas Press, Austin 1980)

[2] M. P. Allen, D. J. Tildesley, *"Computer Simulation of Liquids"*, (Clarendon Press, Oxford 1987)

[3] R. Becker, W. Ludwig, *"Theorie der Wärme"*, (Springer Verlag, 1985)

[4] Ronald Holzlöhner, *"1D-and 2D-Phases of Membranes with Density Perturbations"*, internal paper, (March 1996)

[5] Ronald Holzlöhner, *"Density Perturbations in Mean Field Theory"*, internal paper, (May 1996)

[6] Conversation with C. Jeppesen (UCSB)